Application of Neutron Diffraction in Characterization of Texture Evolution during High-Temperature Creep in Magnesium Alloys

A. Sediako
McGill University, Montreal, PQ, Canada

Contributions from **S. Shook[1], S. Vogel[2], and D. Sediako[3]**
[1] Applied Magnesium International, Denver, CO, USA
[2] Los Alamos Neutron Science Center, Los Alamos, NM, USA
[3] Canadian Neutron Beam Centre, NRC, Chalk River Labs, ON, Canada

Abstract

A good combination of room-temperature and elevated temperature strength and ductility, good salt-spray corrosion resistance and excellent diecastability are frequently among the main considerations in development of a new magnesium alloy for automotive industry. Unfortunately, there has been much lesser effort in development of wrought-stock alloys for high temperature applications. Extrudability and high temperature performance of wrought material become important factors in an effort to develop new wrought alloys and processing technologies. This paper shows some results received in creep testing and studies of in-creep texture evolution for several wrought magnesium alloys developed for use in elevated-temperature applications.

Along with others "traditional" characterization techniques of metals' performance in high-temperature creep, neutron diffraction was employed in this study to analyze evolution of crystallographic texture during creep deformation. The paper compares two methods of texture analysis in neutron diffraction studies: based on monochromatic (reactor-source) beam and white neutron beam (time-of-flight method, synchrotron). The time-of-flight (TOF) spectrometer illuminates the sample with a non-filtered beam of neutrons and captures the readings with an encircled detector array. This provides a very fast and detailed picture of the crystallographic texture for the bulk of the sample. As the white beam retains all neutron wavelengths, it takes much less time to collect statistically-valid dataset for the diffraction pattern.

On the other hand, the monochromatic beam setup includes a monochromatic crystal that filters out a specific wavelength. The diffracted beam is then captured by a much simpler neutron detector. This setup is more flexible, allowing for choosing various wavelengths (depending on the sample material) but obviously requiring more time for statistically viable data collection.

These studies were performed using E3 neutron spectrometer of the Canadian Neutron Beam Centre in Chalk River, ON, and HIPPO TOF spectrometer at Los Alamos Neutron Science Center, NM.

.

1. Introduction

Regardless of enormous efforts put in development of high-strength high-temperature magnesium alloys, the most typical applications of magnesium in automotive use is still limited to a few select applications such as the instrument panel, steering wheel, and valve cover. Limited success was reached in use of magnesium in powertrain applications such as the transmission case and engine block [1, 9]. These applications see service conditions in the temperature range of 150-200^{o}C under 50-70 MPa of tensile and compressive loads. In addition, metallurgical stability, fatigue resistance, corrosion resistance and castability requirements need to be met. More than a decade of research and development has resulted in a number of creep resistant magnesium alloys that are potential candidates for elevated-temperature automotive applications. These alloys are mostly based on rare-earth and alkaline earth element additions to magnesium. A number of alloys are based on additions of Si, Sr, and Ca.

Although a large share of the material used in industry is in the form of castings, the use of wrought products in automotive applications is on the rise. Extruded sections provide opportunities for mass-efficient design of automobile structural and interior components.

One of the main criteria of material performance in automotive high temperature applications is its resistance to creep. However, low resistance to creep deformation at elevated temperatures has been one of the main restricting factors in application of magnesium alloys.

Depending on manufacturing route and resulted grain/crystallographic matrix, wrought magnesium alloys can exhibit quite different behaviour in creep, as compared to similar cast alloys. Several creep-resistant wrought alloys have been studied in [10, 11]. It was shown that magnesium exhibits different creep properties under tension and compression. These studies also show data received in analysis of crystallographic texture and creep-induced residual stress – the factors that would most certainly affect service properties of the material. The targeted alloying groups were magnesium - aluminum – rare earth, magnesium - aluminum – strontium, magnesium - aluminum - calcium, and magnesium - zinc – rare earth. Chemical composition of the analysed samples corresponds to the following alloy designation: AE42, AE33, AX30, AZX310, AJ32, EZ33, and ZE10. Seven alloys targeted in this study were produced by the magnesium division of Timminco Corporation, now Advanced Magnesium International (AMI). The material was cast using a unique controlled-cooling static casting process followed by hot extrusion. All alloys exhibited exceptionally good castability, as well as formability in the extrusion process.

The current analysis is a part of continuing effort to develop low-cost wrought magnesium alloys with improved castability and formability suitable for high temperature applications, as well as to add to understanding of material behaviour in high temperature creep.

2. High-temperature Creep Testing

The received wrought material was subsequently subjected to a tensile creep test at 150^{o}C and 175^{o}C and then to compressive creep test at 150^{o}C under a load of 50 MPa for the duration of

200 hrs. All the samples were creep-tested along the extrusion direction. The following charts illustrate some results of these tests.

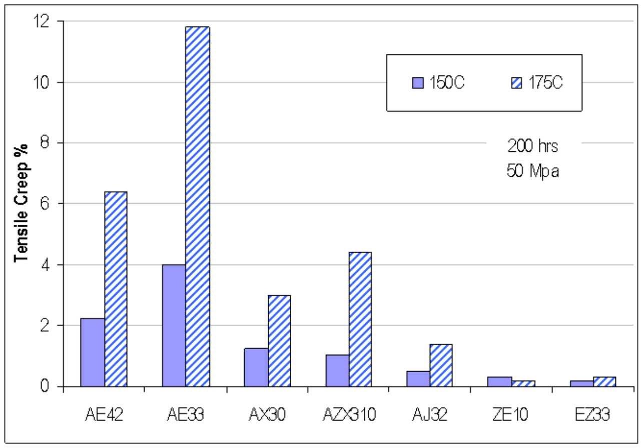

Figure 1 Resistance to creep for the selected alloys at 150 and 175^{o}C

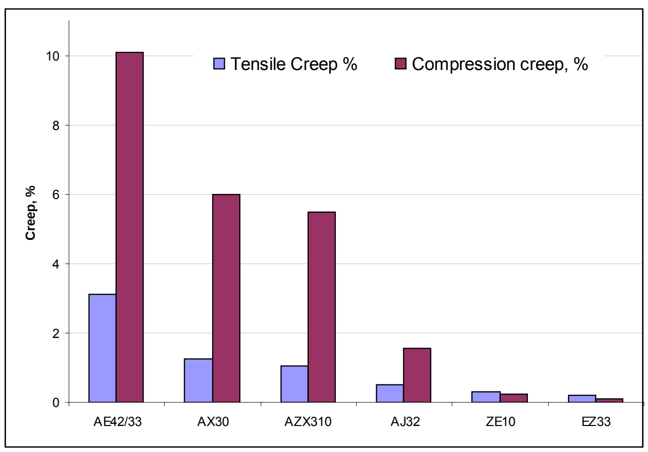

Figure 2 Tension-compression asymmetry in resistance to creep, at 150^{o}C

Data shown in Figure 1 illustrate comparison between results received in the tensile tests at 150^{o}C and 175^{o}C that included both primary and secondary creep. As expected, the 25^{o}C temperature increase lead to significantly reduced resistance to creep, typically by a factor of 3 for all alloys, except ZE10 and EZ33. Evidently, the manufacturing route applied in this study (PMC + hot extrusion) resulted in superior high temperature creep properties for the Mg-Zn-RE alloying system.

This fact was also confirmed in the compressive creep test, performed at 150^{o}C. It is known that typically HCP crystallographic systems exhibit much reduced resistance to creep in compression. This fact can be observed in the following chart, Figure 2, that demonstrates the tension/compression asymmetry in the creep resistance for the studied alloys. Figure 2 indicates that for the identical applied load and duration of the test the resistance to creep was reduced by a factor of 3.5~4 for all of the alloys, but, again, ZE10 and EZ33. It can be concluded from these observations that, compare to the other samples studied in this research, the applied manufacturing route affected favorably the ability of Mg-Zn-RE alloying system to resist the high temperature creep, both in tension and compression. In addition to that, almost no tension-compression asymmetry was observed for the ZE-group samples (in all the tests the resulted creep was within 0.25~0.3% for the ZE10 samples and 0.1~0.2 for EZ33).

Figures 1 and 2 also show that in all tests the AE-group samples exhibited inferior creep properties, compared to the other three alloying systems. This was partially explained in [11] by presence of β-phase $Mg_{17}Al_{12}$, along the grain boundaries in the magnesium matrix that significantly reduced creep resistance at elevated temperatures. A reference was also made on possible effect of initial (i.e. prior to creep) texture.

3. Application of Neutron Diffraction in Material Texture Studies

The comprehensive analysis performed in this study would not be possible without the use of neutron diffraction. The neutron itself, while considered a relatively large particle, does not carry a charge, and therefore is not attracted to any of the other particles inside matter. This lack of attraction to other particles allows the neutron to penetrate deep into a specimen, and retrieve the information that would remain hidden from other testing methods. The test consists of focusing a beam of neutrons onto a particular area of the specimen, and measuring the angle of diffraction.

Using the angle found by neutron diffraction, the distance between the atomic planes can be calculated using a formula referred to as Bragg's Law. Bragg's law is expressed as $n\lambda = 2d\sin\theta$, and is based on the fact that neutrons travel in waves, and relies on the waves' interference.

When using the monochromatic beam setup, neutrons from a nuclear reactor are passed though a monochromatic crystal to separate the "white" (containing many wavelengths) beam into an array with different wavelengths. The neutrons of the selected wavelength are then directed to a specimen. The neutrons that reach the specified location inside the specimen then strike the nuclei and get diffracted from the atomic planes. The diffracted waves leave the material at a certain angle (θ) to the incident beam. If, at this angle, the distance between the planes (d) is equal to a whole number (n) of wavelengths (λ), then there is constructive interference that produces a strong diffraction pattern. This pattern is captured by a detector that moves around the sample, and gathers at what angles the diffraction peaks occur. With such a setup, where the wavelength is pre-set and the angle is measured by the detector, the distance between the atomic planes is found by applying Bragg's Law.

As neutrons get diffracted only from those atomic planes that have correct orientation with regards to the incident beam, for a single crystal or for a coarse-grain material the diffraction intensity may be a strong function of the sample orientation in the beam. For a powder and for a poly-crystal fine-grain material (metals) with a random orientation of crystals the diffraction intensity does not depend on sample orientation with respect to the beam as long as the sampling volume remains the same. This is true for most of metals in as-cast condition solidified under slow cooling rate. This however changes if the material has undergone any form of deformation (stamping, rolling, forging, extrusion, etc.). As a result of deformation many crystals will assume a certain orientation with regards to direction of the deformation. This preferred orientation of crystals forms crystallographic texture of the material. Texture is therefore defined as "the presence of a deviation from the random distribution of grain orientations" [12].

The more the texture develops, the more crystals are aligned in a certain direction. When one rotates such a sample, the peaks change in intensity. By analyzing the deviations between the observed and predicted (random) intensities, it is possible to derive the preferred orientation of the grains. By fully rotating the sample in reciprocal space, while also collecting the neutron diffraction pattern, a texture analysis can be done and diagrams illustrating the strength of the texture can be created.

There is also a different approach to also analyze the texture of metals that is based on the Time-of-Flight method. As neutron wavelength (λ) relates to the time of flight (t) through the following relation: $\lambda = h\, t / (m\, L)$; where ($h$) is Planck's constant, (m) is the neutron's mass, and (L) is the travelled distance. Considering Bragg's law, the following is true:
$\lambda = m\ L\ /\ (h\ t) \ = 2d \sin\theta$. Then, lattice plane spacing is derived as $d = \frac{h}{2mL \sin\theta}\ t$. The parameter ($\frac{h}{2mL \sin\theta}$) is called diffractometer constant (DIFC) and is calculated for each detector tube.

This method is used at Los Alamos national laboratory, New Mexico. The instrument used in this study is called High-Pressure-Preferred-Orientation spectrometer (HIPPO). It uses a particle accelerator to create a white beam of neutrons that is shone at the sample at quick intervals. This much more powerful beam scatters to many angles, which are detected by the complex, encompassing detector arrays (Figure 3). However, without knowing the wavelength, the diffraction intensity at a specific angle provides little information, and this is where the Time-of-Flight method is applied.

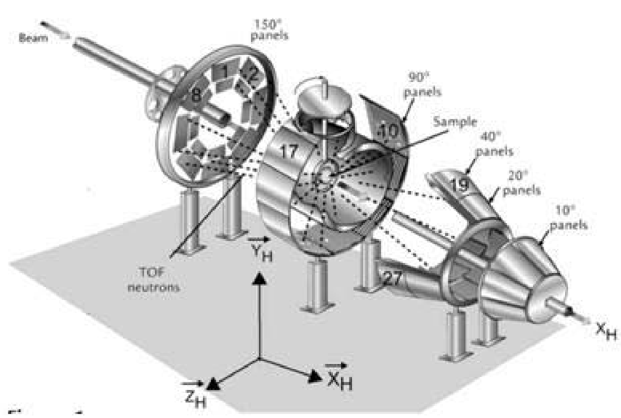

Figure 3 General setup of HIPPO diffractometer at LANL [13]

As the beam is shone at specific intervals, and is caught by the detector at a specific time, the travel time (the time of flight) is known. Using this exact time, and known distance traveled, the speed and wavelength can be determined. This method, while requiring more calculations, and having limited setup space within the detector enclosure, does have many advantages. The “unfiltered” white beam is more powerful as it carries neutrons of all wavelengths, and therefore yields clear and strong diffraction patters much faster than the statistically-viable dataset is collected using the monochromatic beam from a nuclear reactor.

4. Texture Evolution During Creep Deformation

It was also suggested in [11] that the strength of the initial extrusion-type crystallographic texture may be another factor affecting the material resistance to creep. It can be assumed that, considering amount of deformation in creep (up to 10~12% strain), there could be a noticeable texture evolution/modification during the creep testing. These two assumptions were verified in texture analysis performed in HIPPO (High-Pressure-Preferred-Orientation) time-of-flight spectrometer at Los Alamos Neutron Science Center. The time-of-flight method employed by HIPPO for texture analysis is described in detail in earlier study [13].

Similar studies have earlier been performed the monochromatic reactor-source neutron beam at the Canadian Neutron Beam Centre in Chalk River, ON, on pure magnesium and Mg-1.5wt.%Mn samples [14, 15]. It was confirmed that the tested material had gone through significant texture modification in creep testing at 150^{o}C and under the load of 50MPa. A typical “rolling” texture could be observed on the crept specimens. Important conclusions were reached with regards to creep deformation mechanisms for the studied materials.

The following pictures (Figures 4 and 5) show the results of texture calculation using E-WIMF algorithm of the MAUD texture-analysis software [13] based on neutron measurements for several selected alloys.

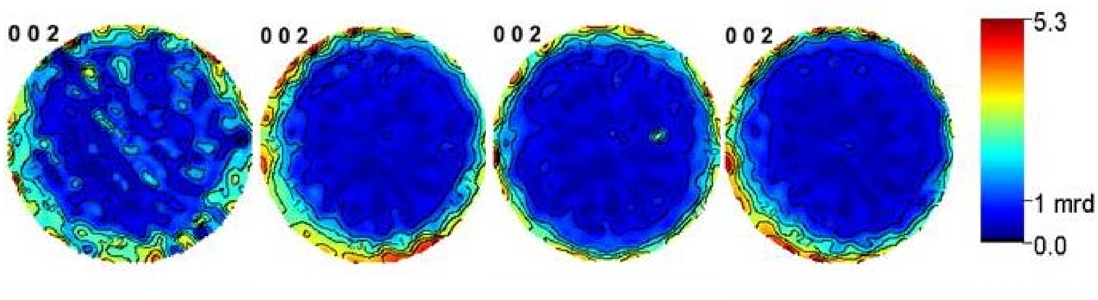

a. – AE42 b. – AJ32 c. – AX30 d. – EZ33

Figure 4 As-extruded texture for selected alloys, (0002) reflection

As expected, Figure 4 indicates that the alloys exhibited typical magnesium extrusion texture with the (0002) poles aligned preferentially normal to the extrusion axis. The basal pole figures have similar strength of the basal texture, ranging from 4.5 m.r.d. (or multiple of random distribution) for AE42 to 5.4 m.r.d. for EZ33.

The Figure 5, however, shows somewhat different intensities for the prismatic $\{10\bar{1}0\}$ orientation for the initial texture and as it modifies as a result of creep deformation. All the samples in Figure 5 were ID'ed in the following manner:

- as-extruded (i.e. not creep tested) – all *a.* samples;
- after compression-creep test, 150^{o}C – all *b.* samples
- after tensile-creep test, 175^{o}C – all *c.* samples

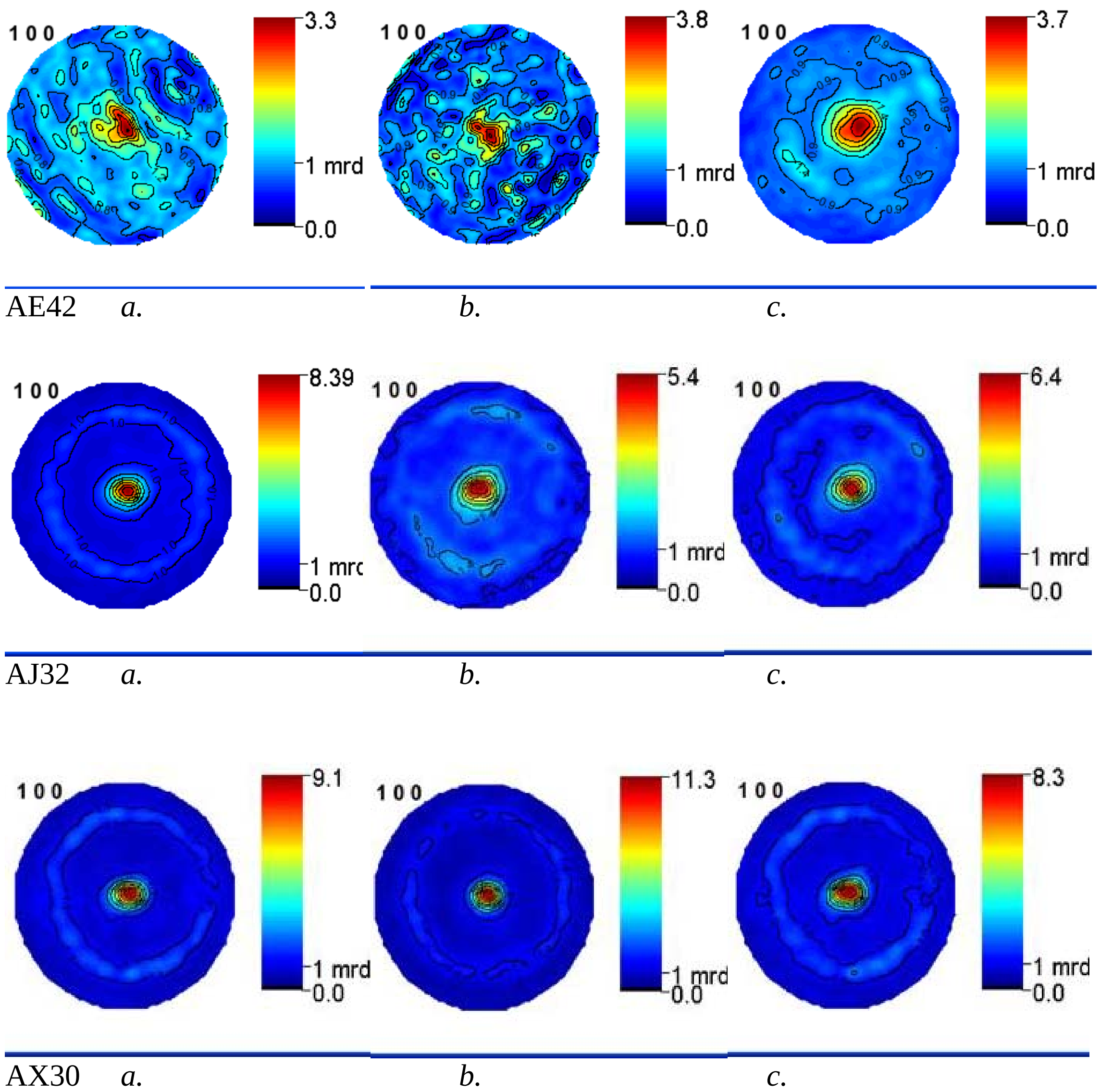

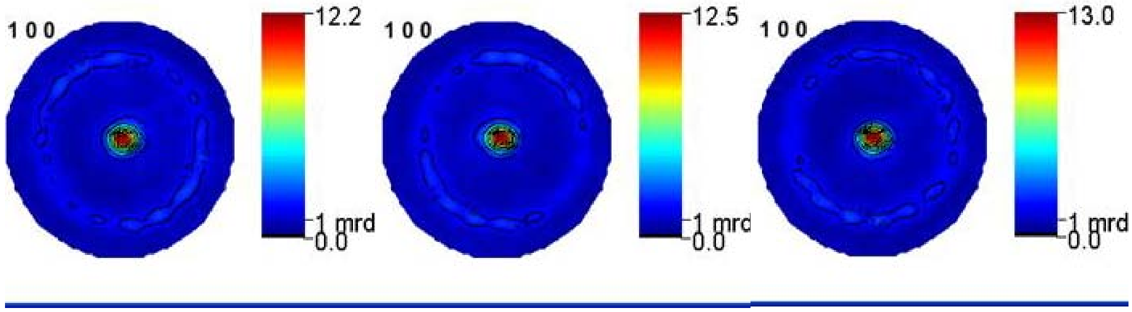

ZE33 *a.* *b.* *c.*

Figure 5 Texture evolution in creep tests for selected alloys, $\{10\bar{1}0\}$ reflection

Figure 5 shows that strength of the initial as-extruded texture for the studied samples can vary for the prismatic reflection $\{10\bar{1}0\}$ pole figures, ranging from ~3 to ~12 m.r.d. Interestingly, the alloys that had relatively weak extrusion texture typically did not fare well in the creep testing (Fig. 1), an observation made earlier in studies [10, 11]. Another observation from Figure 5 is obvious texture modification on the AE42 specimen as a result of creep testing, particularly for the tensile creep specimen (Figure 5, AE42, *c.*). Though strength of the texture remains relatively the same, the grains received further extrusion-type reorientation as the result of tensile creep deformation.

The other three alloys shown in Figure 5 exhibited much lesser texture evolution in creep, which is consistent with the fact that these alloys deformed much less than AE42. Apparently, presence of the $Mg_{17}Al_{12}$ β-phase is only partial reason of inferior performance of AE, AJ, and AX alloys as compared to the EZ-group material.

5. Conclusions

Crystallographic texture studies performed at the Canadian Neutron Beam Centre and Los Alamos Neutron Science Center confirmed that there is a notable difference in the strength of extrusion-type texture for the extruded samples of studied alloys, that represent four alloying systems; namely, Mg-Al-RE, Mg-Al-Ca, Mg-Al-Sr, and Mg-Zn-RE. Two alloys representing the later system developed the strongest texture in the extrusion process (12.3 mrd for the $\{10\bar{1}0\}$ reflection). These alloys also performed the best in the high-temperature creep testing at the temperatures of 150 and 175^{o}C, both under compressive and tensile load. Opposite to that, two alloys from the AE group, developed the weakest texture in the extrusion process (3.3 mrd for the $\{10\bar{1}0\}$ reflection). These alloys also exhibited the lowest resistance to creep in the creep testing.

6. References

[1] Mihriban. O. Pekguleryuz, A. Arslan Kaya, “Magnesium Diecasting Alloys for High Temperature Applications”, Magnesium Technology 2004, Edited by Alan A. Luo, TMS (The Minerals, Metals & Materials Society), 2004, pp. 281-287.

[2] A. A. Luo, Mg Alloys 2003, Mat. Sci.. Forum, Trans Tech, Switzerland, vols. 419-422, 2003, pp. 57-65.

[3] M. Pekguleryuz, P. Labelle, US Pat. No. 6,322,644, Nov 27th, 2001 and PCT WO 01/44529

[4] M. Pekguleryuz, P. Labelle, D. Argo, M. Dierks, T. Sparks, T. Waltematte, World Magnesium Conference, IMA, Brussels, May 2001, pp. 27-33.

[5] M. Pekguleryuz, P. Labelle, E.Baril, D. Argo, SAE Paper 2003-01-190, Detroit, 2003.

[6] S. Koike, K. Wasizu, S. Tanaka, T. Baba and K. Kikawa, SAE Paper 2000-01-1117, Detroit, March, 2000.

[7] E.Aghion, B.Bronfin, H.Friedrich, S.Schumann, F. von Buch., 2003 Magnesium Technology, TMS, San Diego, March 2003, pp. 177-182.

[8] M. Lefebvre, M. Pekguleryuz, P. Labelle, US Pat. No 6, 342,180, Jan 29, 2002 and PCT WO 02/099147

[9] A. Luo, M. Balough, B. R. Powell, SAE Paper 2001-01-0423, Detroit, Michigan, 2001.

[10] S. Shook and D. Sediako, “Analysis of Stress Evolution in High Temperature Creep Testing of Creep-Resistant Magnesium Alloys”, 66th Annual World Magnesium Conference, San Francisco, California, 2009, pp. 43-51.

[11] D.Sediako, S. Shook, “Application of Neutron Diffraction in In-situ Studies of Stress Evolution in High Temperature Creep Testing of Creep-Resistant Magnesium Alloys”, The Minerals, Metals & Materials Society, TMS, San Francisco, CA, February, 2009, Magnesium Technology 2009, pp. 255-259.

[12] M. De Graff, M.E. McHenry, “Structure of Materials: An Introduction to Crystallography, Diffraction, and Symmetry”, Cambridge University Press, 2007, 844 p.

[13] H.-R.Wenk, L. Lutterottia, and S. Vogel, “Texture analysis with the new HIPPO TOF diffractometer”, Nuclear Instruments and Methods in Physics Research Section A: Accelerators, Spectrometers, Detectors and Associated Equipment, Volume 515, Issue 3, 11 December 2003, pp. 575-588.

[14] M. Çelikin, F. Zarandi, D. Sediako, M.O. Pekguleryuz, “Compressive Creep Behavior of Cast Magnesium under Stresses above the Yield Strength and the Resultant Texture Evolution”, Canadian Metallurgical Quarterly, Vol. 48, No.4, 2009, pp. 419-432.

[15] M. Çelikin, D. Sediako, and M. Pekguleryuz, "Effect of Compressive Creep-Deformation on the Crystallographic Texture of - Pure Mg and Mg-Mn Casting

Alloys", The Minerals, Metals & Materials Society, TMS, Seattle, WA, February, 2010, Magnesium Technology 2010, pp. 249-251.